

A 1.2mW/channel 100m-Pitch-Matched Transceiver ASIC with Boxcar-Integration-Based RX Micro-Beamformer for High-Resolution 3D Ultrasound Imaging

Guo, Peng; Fool, Fabian; Noothout, Emile; Chang, Zu-Yao; Vos, Hendrik J.; Bosch, Johan G.; Verweij, Martin D.; de Jong, Nico; Pertijs, Michiel

DOI

[10.1109/ISSCC42614.2022.9731784](https://doi.org/10.1109/ISSCC42614.2022.9731784)

Publication date

2022

Document Version

Accepted author manuscript

Published in

2022 IEEE International Solid-State Circuits Conference, ISSCC 2022

Citation (APA)

Guo, P., Fool, F., Noothout, E., Chang, Z.-Y., Vos, H. J., Bosch, J. G., Verweij, M. D., de Jong, N., & Pertijs, M. (2022). A 1.2mW/channel 100m-Pitch-Matched Transceiver ASIC with Boxcar-Integration-Based RX Micro-Beamformer for High-Resolution 3D Ultrasound Imaging. In L. C. Fujino (Ed.), *2022 IEEE International Solid-State Circuits Conference, ISSCC 2022: Digest of technical papers* (pp. 496-498). Article 9731784 (Digest of Technical Papers - IEEE International Solid-State Circuits Conference; Vol. 2022-February). IEEE. <https://doi.org/10.1109/ISSCC42614.2022.9731784>

Important note

To cite this publication, please use the final published version (if applicable).
Please check the document version above.

Copyright

Other than for strictly personal use, it is not permitted to download, forward or distribute the text or part of it, without the consent of the author(s) and/or copyright holder(s), unless the work is under an open content license such as Creative Commons.

Takedown policy

Please contact us and provide details if you believe this document breaches copyrights.
We will remove access to the work immediately and investigate your claim.

32.3 A 1.2mW/channel 100 μ m-Pitch-Matched Transceiver ASIC with Boxcar-Integration-Based RX Micro-Beamformer for High-Resolution 3D Ultrasound Imaging

Peng Guo¹, Fabian Fool¹, Emile Noothout¹, Zu-Yao Chang¹, Hendrik J. Vos^{1,2}, Johan G. Bosch², Martin D. Verweij^{1,2}, Nico de Jong^{1,2}, Michiel A. P. Pertijs¹

¹Delft University of Technology, Delft, The Netherlands, ²Erasmus MC, Rotterdam, The Netherlands

The integration of 2-D ultrasonic transducer arrays and pitch-matched ASICs has enabled the realization of various 3-D ultrasound imaging devices in recent years, e.g. [1-3]. As applications such as 3D intravascular ultrasonography, intra-cardiac echocardiography and trans-fontanelle ultrasonography call for miniaturization and improved spatial resolution, higher frequency transducers (> 5MHz) with a correspondingly smaller array pitch (< 150 μ m) are needed. Such devices generally employ a large number of transducer elements, calling for channel-count reduction in the ASIC while meeting stringent restrictions on per-element power consumption and die area. Micro-beamforming (μ BF) is an effective way of reducing channel count by performing a delay-and-sum operation on the echo signals received within a sub-array [1]. However, prior μ BF implementations employ per-element capacitive memory to realize the delay [1,2], making it increasingly difficult to apply μ BF in smaller-pitch arrays.

This paper presents a μ BF architecture that employs current-mode summation and boxcar integration to realize delay-and-sum on an N -element sub-array using $N\times$ fewer capacitive memory elements than conventional μ BF implementations. This facilitates the use of μ BF in smaller-pitch applications, as demonstrated by a prototype transceiver ASIC targeting a wearable ultrasound device that monitors brain perfusion in preterm infants via the fontanel (Fig. 1). To meet its strict spatial resolution requirements, a 10-MHz 100- μ m-pitch piezoelectric transducer array is employed, leading to a per-element die area $>2\times$ smaller than prior designs employing μ BF [1-3].

Conventional μ BF implementations [1,2] sample the echo signals $V_{1..N}$ from the sub-array elements and store the last K samples for each element, thus requiring K capacitive memory cells per element (Fig. 1). These stored values are then read out after a programmable time delay and added in the voltage- or charge-domain to implement the delay-and-sum operation. The proposed μ BF, in contrast, operates on current-mode input signals $I_{1..N}$, and successively connects these to a set of K memory cells. These collect charge representing the upcoming K output samples, allowing summation to take place in the current-domain at their input. The delay associated with an individual input is set by the delay between the connection of that input to a memory cell, and the moment that the memory cells connects to the output. This architecture reduces the number of memory cells by a factor of N compared to conventional μ BFs [1,2]. In contrast with prior current-mode μ BFs, which either employ per-channel delay lines [4] or explicit per-channel S/H stages [5], the signal currents are directly integrated on the memory capacitors, realizing boxcar integration that provides inherent anti-alias filtering and obviates the need for such filtering in the analog front-end (AFE), thus further reducing die size.

Fig. 2 shows a block diagram of the prototype ASIC interfacing with an 8 \times 8 transducer array. Element-level high-voltage (HV) pulsers allow all elements to contribute to acoustic pulse transmission (TX), with the ability to define time delays at the row- or column-level to steer the resulting TX beam to different angles. For echo reception (RX), the array is divided into sub-arrays of 2 \times 2 elements. After TX, HV T/R switches and multiplexers connect two of these sub-arrays to the receive (RX) circuitry. The signal currents from the elements of the selected sub-arrays are amplified by 4 AFEs and then fed, via multiplexers that set the element delays, to 4 memory cells, implemented as active boxcar integrators to improve linearity compared to a passive integrator. Output sample-and-hold (S/H) stages drive the μ BF outputs off chip.

The AFEs are based on the design presented in [6] and consist of a capacitive-feedback transimpedance amplifier (TIA), the output of which is capacitively coupled to the input of a current amplifier (CA). The CA provides a high-Z output to drive the boxcar integrator in the μ BF with an amplified version of the transducer's signal current. The AFE's gain can be continuously controlled in a range of 36dB by an external voltage V_{TGC} to provide time-gain compensation, i.e. to compensate for the stronger attenuation of echoes that arrive later. The AFE provides less than ± 0.4 dB gain error and has a 1.31pA/ $\sqrt{\text{Hz}}$ input-referred noise density within 6MHz to 14MHz bandwidth at its maximum gain ($V_{TGC} = 1.1\text{V}$).

Fig. 3 shows the detailed implementation of the μ BF. To set the delay profile, each of the input currents $I_{1..4}$ is connected to one of 6 summation nodes, which correspond to 6 possible delay steps. These 6 summation nodes are cyclically connected to the 4 boxcar integrators, orchestrated by an 80-MHz delay clock $\text{CLK}_{\text{delay}}$. The active boxcar integrators alternate between integration ($R_i = 0$) and readout ($R_i = 1$) phases. During the latter, the accumulated charge is transferred to one of two S/H stages, which operate in a ping-pong fashion and alternately drive the output, controlled by a 40-MHz clock CLK_{SH} . While $\text{CLK}_{\text{delay}}$ sets the minimum delay step to 12.5ns and the delay range to 62.5ns, CLK_{SH} , independently, sets the output sampling period to 25ns. The boxcar integration time is 25ns to provide effective anti-alias filtering.

The OTAs in the boxcar integrators and S/H stages are implemented using inverter-based amplifiers (Fig. 4) with current-reuse supply- and ground-regulators that suppress interference and are shared at the sub-array level to save area. Two capacitive level shifters (C_1/C_2) are used to enlarge the dynamic range of the OTAs. These are reset during the TX period (Φ_{TX}) and hold the DC bias points during the RX period (Φ_{RX}).

The ASIC has been fabricated in a 180nm BCD process (Fig. 7) and consumes 1.2mW/channel, of which 0.8mW is consumed by the AFE and 0.33mW by the μ BF, while the 30-V TX consumes 32 μ W/channel at a pulse repetition frequency of 10kHz. Fig. 4 shows the input-referred noise at the μ BF's output (Fig. 4) for different TGC control voltages (V_{TGC}). At the highest gain, it achieves 0.67pA/ $\sqrt{\text{Hz}}$, which is close to half of the input referred noise (1.31pA/ $\sqrt{\text{Hz}}$) of a single-channel AFE measured at CA's output. This factor is in line with the $\sqrt{N} = 2$ noise reduction expected from a μ BF without noticeable noise-folding effects and is maintained across the full gain range (Fig. 4). The gain of the full signal chain at 7 different TGC levels (Fig. 5) shows a minimum -3dB bandwidth of 14.7MHz at $V_e = 1.1\text{V}$. A measurement of SNR vs. input current shows a peak SNR of 54 dB, and a 82 dB dynamic range. Accurate delay-and-sum operation is demonstrated by applying time-shifted sinusoidal inputs to the chip, thus emulating acoustic inputs arriving at different angles, and comparing the μ BF response with the ideal expected directivity for different μ BF delay settings. The HV pulsers successfully produce 30-V pulses with a delay resolution of 12.5ns.

Acoustic characterization has been done on a prototype with transducer array built on top as shown in Fig. 7. A small water tank was mounted on top of the chip, with 3 needle reflectors positioned at about 8mm from the transducer surface (Fig. 6). For TX, 3-cycle 30-V pulses were used. The μ BFs were steered to different angles and the amplitude of the received echo signals increases as the μ BF steered towards the reflectors. A B-mode image clearly shows the needles positions even with the small aperture size (0.8mm \times 0.8mm).

A comparison with prior μ BF ASIC designs with pitch-matched 2D arrays (Fig. 7) shows that this work achieves the smallest array pitch, the highest center frequency, and the smallest μ BF area per channel, making the proposed μ BF architecture a promising solution for channel-count reduction in next-generation small-pitch 3D ultrasound imaging devices.

Acknowledgement:

This work is part of the MIFFY project (#15293) funded by the Open Technology Programme of the Dutch Research Council NWO.

References:

- [1] C. Chen, et al., 'A Pitch-Matched Front-End ASIC With Integrated Subarray Beamforming ADC for Miniature 3-D Ultrasound Probes', IEEE JSSC, vol. 53, no. 11, pp. 3050–3064, Nov. 2018.
- [2] Y. Igarashi, et al., 'Single-Chip 3072-Element-Channel Transceiver/128-Subarray-Channel 2-D Array IC With Analog RX and All-Digital TX Beamformer for Echocardiography', IEEE JSSC, vol. 54, no. 9, pp. 2555–2567, Sep. 2019.
- [3] M.-C. Chen, et al., 'A Pixel Pitch-Matched Ultrasound Receiver for 3-D Photoacoustic Imaging With Integrated Delta-Sigma Beamformer in 28-nm UTBB FD-SOI', IEEE JSSC, vol. 52, no. 11, pp. 2843–2856, Nov. 2017.
- [4] B. Stefanelli, et al., 'An analog beam-forming circuit for ultrasound imaging using switched-current delay lines', IEEE JSSC, vol. 35, no. 2, pp. 202–211, Feb. 2000.
- [5] J.-Y. Um, 'Current-mode ultrasound beamformer with multiple-input-sequential-output memory structure', Electronics Letters, vol. 54, no. 9, pp. 545–546, May 2018.
- [6] P. Guo, et al., 'A Pitch-Matched Analog Front-End with Continuous Time-Gain Compensation for High-Density Ultrasound Transducer Arrays', in Proc. Eur. Solid-State Circuits Conf. (ESSCIRC), Sep. 2021, pp. 163–166.

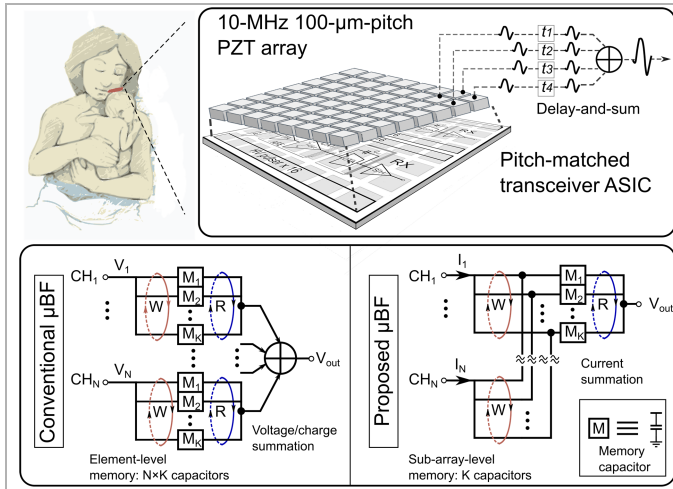


Figure 32.3.1: Overview of the ASIC for trans-fontanelle echography and comparison between conventional and proposed micro-beamforming

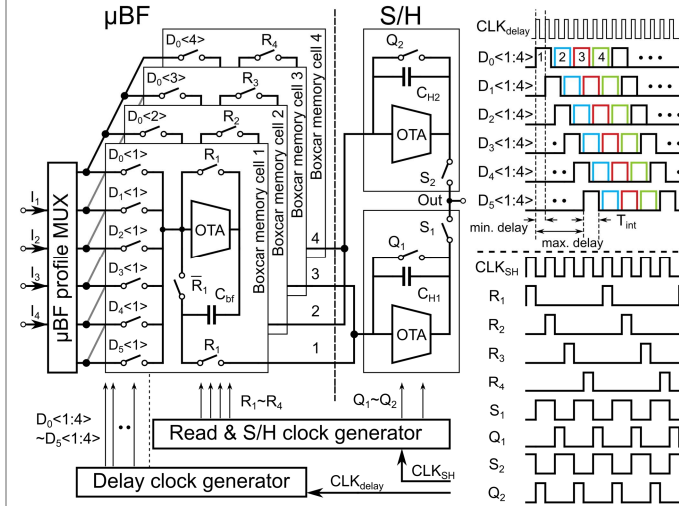


Figure 32.3.3: Circuit diagram of the boxcar-integration μBF , the ping-pong S/H and their timing details

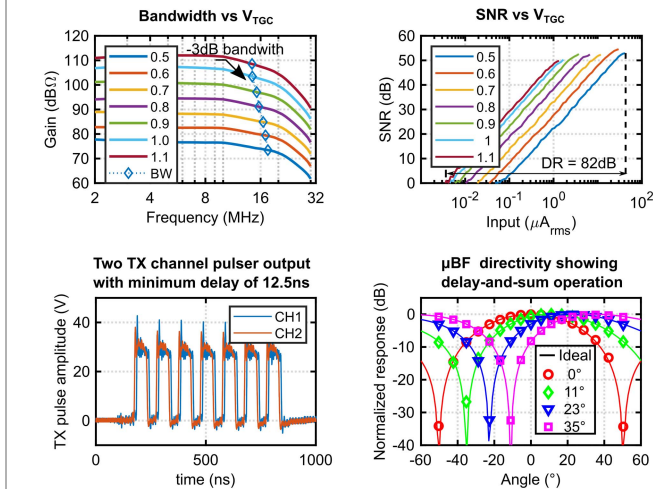


Figure 32.3.5: Measured signal-chain bandwidth, signal-to-noise ratio, high-voltage TX pulser and μBF beamforming directivity

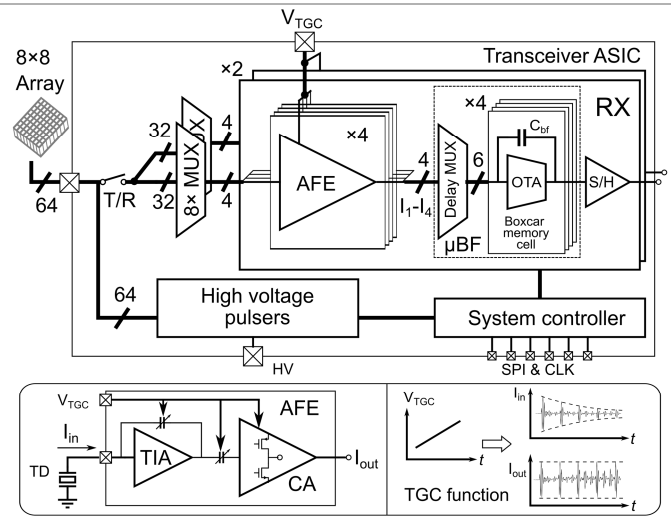


Figure 32.3.2: ASIC architecture with an inset showing the continuous-time time-gain-compensation AFE

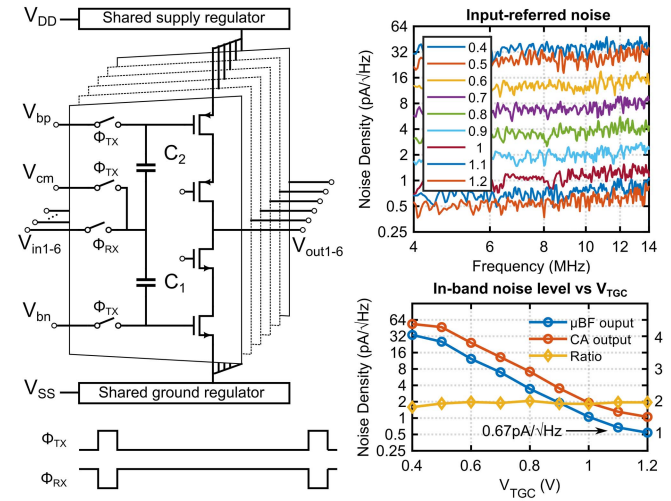


Figure 32.3.4: The inverter-based amplifiers, measured input-referred noise of the μBF and noise reduction ratio of the μBF

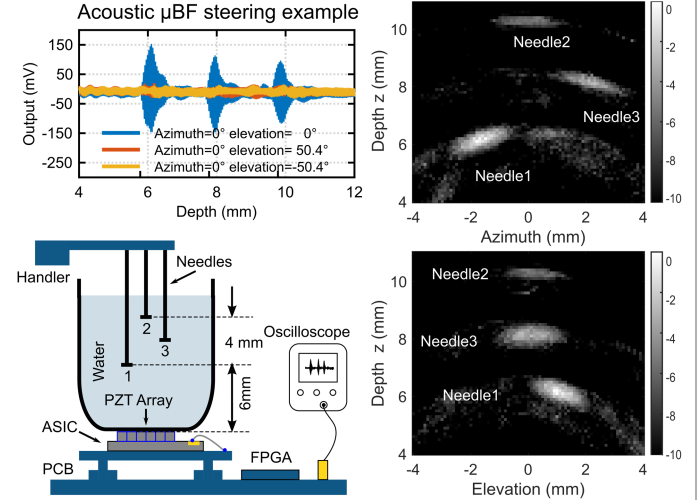


Figure 32.3.6: Acoustic beam-steering example, acoustic measurement setup and B-mode images

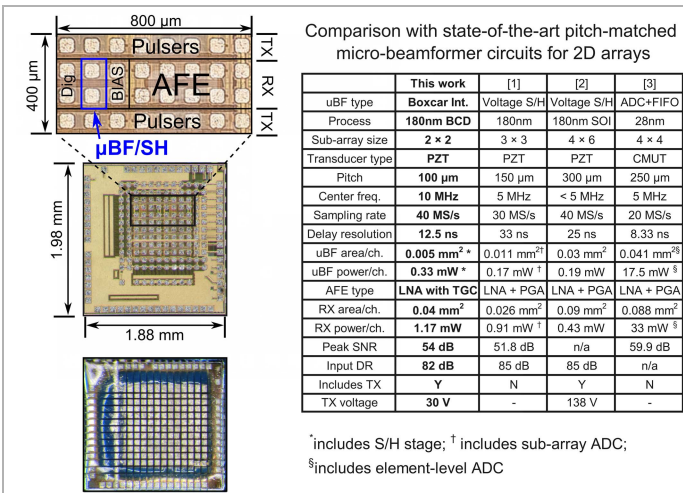


Figure 32.3.7: Micrograph of the ASIC and the prototype with transducers on top and comparison with the state-of-art